

Fig. 2 SDS-PAGE of SN chimeras. Purified chimeric proteins were tested for association in SDS-PAGE and stained with Coomassie brilliant blue. M is the molecular weight standard. Positions of monomer, dimer and trimer are marked on the right.

onance (NMR) studies of the helical peptide, we find that the hydrogen bonding properties of the asparagine side chain are well modeled by the interactions seen in soluble leucine zippers. It is evident that asparagines provide a strong free energy of association by forming interhelical hydrogen bonds in a hydrophobic environment.

Design of the transmembrane helices

Transmembrane helices were designed based on the GCN4 leucine zipper motif to test if the soluble protein dimer interface, with or without a polar residue (Asn), could mediate transmembrane helix association. Since the 33-amino acid GCN4 leucine zipper is longer than average transmembrane helices, only residues 9–31 were chosen in the design. The sequence design includes residues at positions *a* and *d* in the GCN4 leucine zipper and replaces the remaining residues with leucines, the most abundant residue in TM helices^{15–17}. The names of the chimeric proteins and synthetic peptide used in this study represent residues at successive *a* positions, where deviations from a poly-leucine helix occur. Thus, VNVV is the leucine zipper motif, whereas LLLL is poly-leucine. Controls for dimerization include the GpA TM helix, which has been shown to dimerize strongly, and a poly-leucine helix, which provides a measure of background association in the absence of the leucine zipper interface. In another control helix, the asparagine in the design sequence is replaced by a valine to evaluate the contribution of this polar residue to helix association.

Helix association in a detergent environment

Studies using the staphylococcal nuclease (SN) chimera system have been successful in defining the GpA and phospholamban TM helical interfaces by analyzing the ability of mutants to form oligomers during sodium dodecyl sulfate (SDS) polyacrylamide gel electrophoresis (PAGE)^{3–5,18}. In our study, the designed TM helices were fused after a flexible linker to the C-terminus of SN to form chimeric proteins (Fig. 1b). These nuclease chimeras were expressed in *Escherichia coli*, and purified in the presence of detergent.

Purified chimeric proteins were tested for their ability to associate during SDS-PAGE (Fig. 2). The chimeric proteins migrate with an apparent molecular mass of either 21 kDa or 42 kDa, corresponding to the monomeric and dimeric species, respectively. The LLLL and VVVV chimeras migrate as monomers, whereas the VNVV chimera shows approximately equal amounts of dimer and monomer. The control GpA chimera is dimeric. Remarkably, while a poly-leucine helix does not dimerize under the experimen-

tal conditions used here, introduction of only four residues at the *a* positions from the GCN4 leucine zipper motif, Val, Asn, Val and Val, into this poly-leucine sequence induces dimerization. In contrast, a construct with valines occupying all four *a* positions (VVVV) migrated exclusively as a monomer, identical to LLLL. These results indicate that valines alone are not sufficient and that the asparagine is required for dimerization in detergent micelles.

Competition experiments were performed to test if the TM helical segment of the chimera was responsible for the observed dimerization. A 28-residue peptide (3.3 kDa) including the VNVV TM sequence (Fig. 1b) was mixed with the VNVV SN chimeric protein in the SDS-PAGE assay (Fig. 3). The homodimer of the chimera is disrupted even at a low peptide:chimera ratio (lane 3), and the extent of disruption increases with increasing concentration of the peptide. As the homodimer disappears, two additional bands appear above the monomer. Based on their apparent mass and spacing, they are interpreted as heterodimers and heterotrimers composed of one chimera and two peptides. The above observation indicates that association of chimeras is mediated by the designed transmembrane helix and is reversible under these experimental conditions. To confirm that the interaction with the peptide requires the motif residues of VNVV, competition experiments using the VNVV peptide were performed on the LLLL, VNVV, VVVV and GpA chimeras. Samples were analyzed using SDS-PAGE (Fig. 4). All chimeras except VNVV retain their original oligomerization states upon addition of the peptide. The fact that the VNVV peptide is only able to associate with the VNVV chimera but not with other similar proteins strongly suggests that the interactions involve the motif residues in the TM region of the protein. It should be mentioned that a homotrimer of the VNVV chimera was not observed in the SDS-PAGE analysis, perhaps due to steric interference between the nuclease domains in the trimeric state.

To further probe the association interface, the valines at the *a* positions in the VNVV chimera were substituted for leucines, resulting in five new chimeras (LNVV, VNVL, LNVL, VNLL, and LNLL). Partially purified forms of these chimeras show a dimerization propensity comparable to that of VNVV in SDS-PAGE (results not shown). Therefore, it can be concluded that in SDS micelles the valines in the leucine zipper motif do not necessarily constitute a better dimerization interface than leucines. In fact, asparagine alone in a poly-leucine helix is sufficient to mediate dimerization.

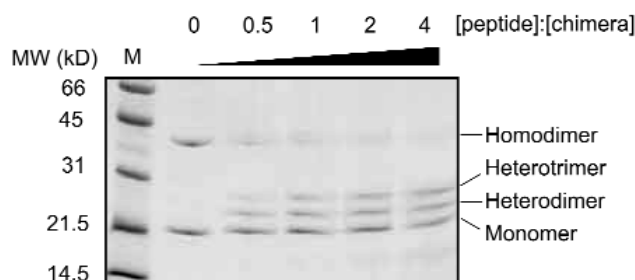


Fig. 3 Competition experiment with VNVV peptide. Purified SN chimera of VNVV was mixed with VNVV peptide at a peptide:chimera molar ratio of 0, 0.5, 1, 2 and 4, respectively. Samples were tested for disruption of chimera homodimer by the peptide in SDS-PAGE. M is the molecular weight standard. Positions of monomer and homodimer of the chimera, heterodimer and heterotrimer of the chimera and peptide are marked on the right. No band was observed in the gel beyond the area shown.

articles

Helix association in a biological membrane

To test whether the observed association in SDS-PAGE can also occur in a membrane, the transmembrane designs were examined in an *in vivo* system (TOXCAT) previously developed to evaluate association of chimeras in the *E. coli* inner membrane¹⁰. Each chimeric protein is composed of the cytoplasmic ToxR transcription activation domain (ToxR') at its N-terminus, the designed transmembrane helix and the periplasmic maltose binding protein domain (MBP) at its C-terminus (Fig. 1b). The parallel association of the chimera that is mediated by the transmembrane sequence brings the ToxR activation domains in close proximity, thereby activating the expression of the reporter gene, chloramphenicol acetyltransferase (CAT)¹⁹. The level of CAT activity (representing the amount of CAT expression) in cell lysates has been shown to correlate with the extent of TM helix association¹⁰. A set of shortened forms of the designed TM sequences was subcloned as TOXCAT chimeras (Fig. 1b), of which VN and NN were made to further study the role of asparagine in promoting association of these TM helices.

The CAT activity from cells expressing chimeras of designed TM relative to that of GpA is shown in Fig. 5. Since the extent of chimera association depends on the concentration of protein in the membrane, the chimera expression levels were detected by immunoblots and quantified by densitometry. The variations in expression between chimeras were small (less than 36%) and the calculation of the relative CAT activities was adjusted accordingly.

The LL and VV chimeras induced CAT expression much less than the GpA TM. CAT expression induced by the NV and VN chimeras, however, surpassed that of the GpA TM. These results are consistent with those obtained from SDS-PAGE of nuclease chimeras, except that in SDS micelles GpA dimerizes better than VNVV. This discrepancy may be due to binding effects in SDS micelles. It has been noticed in previous studies that mutations to polar residues in the GpA TM helix disrupted dimerization in SDS micelles but not in the TOXCAT assay in a biological membrane^{4,10}. Interestingly, NN induces twice the CAT activity as NV or VN, suggesting that the contribution of asparagines to the helix association is independent of the rest of the helix. The above observations were confirmed independently in disk diffusion assays (results not shown), which measure CAT expression by quantifying chloramphenicol resistance acquired by host cells¹⁰. All chimeras appear to be membrane associated as determined by the ability of their host cells to grow on plates containing maltose as the only carbon source, indicating active MBP on the periplasmic side of membrane, and by the localization of the chimeras in membrane fractions (results not shown). These results support the interpretation that the designed TM helices are able to associate in a biological membrane as well as in SDS micelles, and that they can do so in a parallel orientation.

Leucine zipper has insufficient packing interactions

Soluble leucine zippers with leucines at both *a* and *d* positions are able to associate^{20–25} to form either dimers or trimers. In our system an interface composed only of leucines induces substantially weaker dimerization in both SDS-PAGE and TOXCAT assays, compared to the GpA and VNVV helices. It has been reported recently that a poly-leucine helix was able to self-assemble more efficiently than a water-soluble poly-alanine helix in membranes as well as in detergent²⁶. The authors attributed the ability to dimerize to complementary surfaces formed by the leucine side chains. Without comparing the poly-leucine result to a positive standard, their interpretation of the magnitude of dimerization might be misleading. Our studies suggest that the complemen-

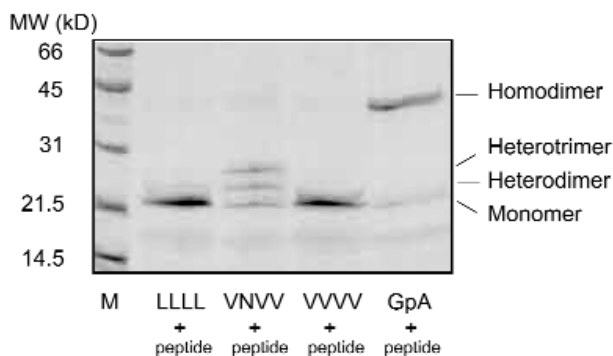


Fig. 4 Interactions between SN chimeras and VNVV peptide. Purified chimeric proteins were mixed with the VNVV peptide at a peptide:chimera molar ratio of 4:1. Samples were tested for interactions between the chimeras and peptide. M is the molecular weight standard.

tary surface of a leucine zipper is probably insufficient to generate enough interhelical packing interactions required for a stable oligomer in a membrane. This idea is further supported by our observation that the VVVV interface, which mediates association of soluble leucine zippers^{20,27}, did not induce a higher level of transmembrane helix association than LLLL both in detergent micelles and in a biological membrane. In aqueous solution, the folding of such leucine zipper interfaces largely results from the hydrophobic effect, in addition to packing (van der Waals) interactions. The two-stage model of transmembrane helix association suggests that we can isolate the contribution of the hydrophobic effect from that of packing; these two factors are often inseparable in the case of soluble proteins because the polypeptide cooperatively folds from a random coil to a tertiary structure. Since transmembrane helices are individually stable, the fundamental question of helical membrane protein folding is to ask what forces drive the association of these helices. Helical association in a membrane is the result of energetic gains from helix–helix and lipid–lipid interactions, minus the loss of helix–lipid interactions.

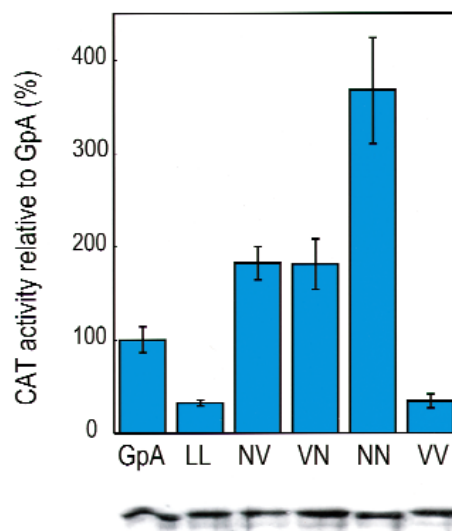


Fig. 5 TOXCAT assays of transmembrane helix association. Cells expressing TOXCAT chimeras were lysed and assayed for CAT activity. All values are the average of three independent samples with the error bar showing the estimated standard deviation. Expression levels of chimeras were estimated from immunoblots (bottom) and were taken into account in the calculation of the relative CAT activity.

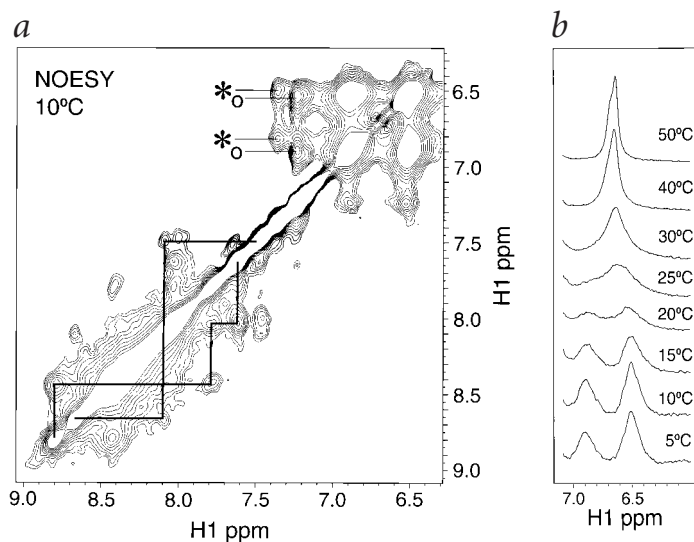


Fig. 6 Proton NMR spectra of the synthetic membrane leucine zipper. **a**, Helical connectivities between amide signals are drawn on a NOESY (10 °C, 35 ms mixing time) spectrum (800 MHz). * and ○ indicate NOE cross peaks from alternate conformations of the Asn side chain. **b**, Downfield sections of one-dimensional NMR spectra collected at increasing temperatures (500 MHz).

Secondary structure and asymmetric H-bonding

Proton NMR data collected on the synthetic peptide (VNVV) in an SDS micellar environment reveal information on the Asn side chain and helical secondary structure near that position. Since there are no aromatic side chains, the peaks between 6 and 9 p.p.m. in Fig. 6a are from protons bound to nitrogens (that is, backbone and the single asparagine side chain amide). The asparagine side chain Nδ protons are assigned as the most upfield of the amide resonances 6.5 and 6.9 ppm. At low temperatures, two broad Asn side chain peaks are found. Nuclear Overhauser effect spectroscopy (NOESY) data collected at 10 °C show distinct NOE patterns for each side of the broad asparagine peaks to amide (* and ○, Fig. 6a) and aliphatic resonances. Thus the two peaks contain four signals, indicating that the asparagines exist in two populations at this temperature. As the temperature is raised, the two sets of overlapping peaks shift toward each other, coalesce and sharpen (Fig. 6b) to give one set of conformationally averaged asparagine signals where the H_Z (syn) and H_E (anti) resonances practically overlap. The coalescence temperature is ~10 °C higher at 800 MHz (not shown) compared to 500 MHz; this field dependence confirms that the temperature induced changes seen in these peaks are a result of conformational exchange.

Circular dichroism (CD) data collected on a diluted NMR sample (Fig. 7) of the synthetic peptide (VNVV) in SDS show a very high degree of helical secondary structure that does not melt between 10 and 90 °C. In contrast, soluble leucine zippers that contain an asparagine do unfold within this range. However, a direct comparison of the soluble with the membrane leucine zippers is complicated by the detergent environment that generally affords membrane helices greater thermal stability. While the melting of soluble proteins measured by CD is frequently correlated with a loss of tertiary structure, it is entirely possible that the helical interfaces of membrane proteins denature without significantly affecting the secondary structure in a micelle or lipid bilayer environment.

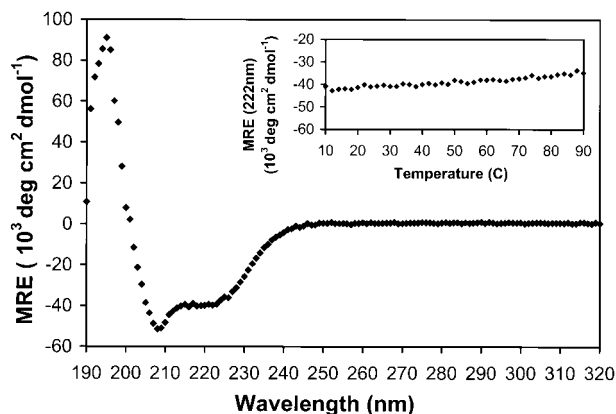


Fig. 7 CD of the synthetic membrane peptide VNVV in SDS micelles. The mean residue ellipticity (MRE) of the peptide shows strong helical secondary structure. The inset shows the MRE at 222 nm with increasing temperature.

It has been shown that specific packing is a key feature of the GpA transmembrane helix, where the complementary interface is preformed by side chains in their ideal helical rotomers, with minimal cost of conformational entropy upon dimerization⁸. Alternatively, additional association energy may be gained by interhelical polar interactions.

Asparagine provides helix association energy

In solution, Asn residues at leucine zipper interfaces are thought to help define helix association specificity even though they do so at the expense of stability^{20,25,27–29}. However, it is not clear how a polar group at the transmembrane helix interface would affect the association of helices in a hydrophobic environment. Our results showed that the asparagine of the GCN4 leucine zipper motif, in an otherwise poly-leucine helix, is able to drive the helical association in detergent micelles. In a study of a similar design, asparagine was also found to be key in oligomer formation in detergents using ultracentrifugation and fluorescence resonance energy transfer³⁰. Using TOXCAT, we have further established that association can occur in a biological membrane. Moreover, in the TOXCAT studies the NN chimera showed twice the dimerization signal as NV or VN, indicating that the asparagines are independently involved in the association and that adding an asparagine increases the stabilizing energy. It should be noted that we have observed multiple oligomeric species for the VNVV helix, indicating a lack of oligomerization specificity (Figs 3,4). In solution three-stranded leucine zippers coexisting with their dimeric counterparts have been observed for some natural and engineered systems^{20,31–34}. Although the hydrophobic residues at the interfaces of leucine zippers make excellent packing interactions, they do not provide sufficient specificity to determine a unique oligomeric state. In solution, this lack of specificity is frequently compensated for by the incorporation of polar residues at the interface that may form hydrogen bonds (position *a*) or salt bridges (positions *e* and *g*). However, polar residues are much less common in transmembrane helices and their structural and biological roles are poorly understood. Our results suggest that in a hydrophobic environment asparagine provides stability rather than oligomerization specificity. This can be explained by the substantially larger free energy gain in formation of an interhelical hydrogen bond in a low dielectric environment than that in an aqueous solution, where polar side chains can form alternative interactions with water.

articles

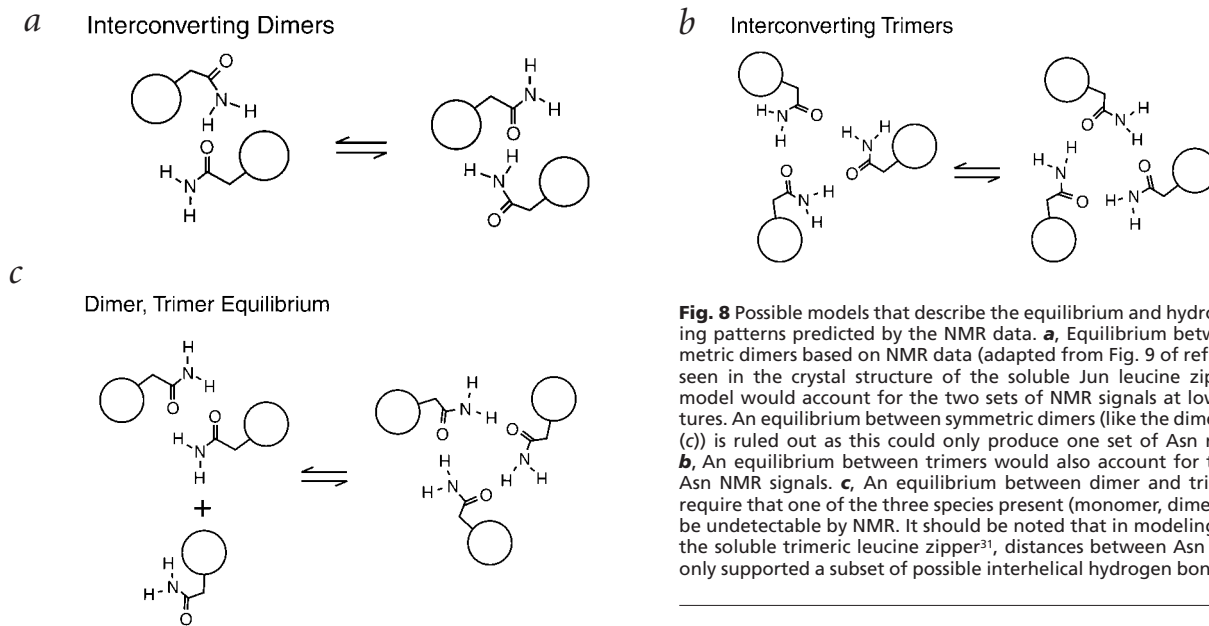


Fig. 8 Possible models that describe the equilibrium and hydrogen bonding patterns predicted by the NMR data. **a**, Equilibrium between asymmetric dimers based on NMR data (adapted from Fig. 9 of ref. 35) and as seen in the crystal structure of the soluble Jun leucine zipper¹⁴. This model would account for the two sets of NMR signals at low temperatures. An equilibrium between symmetric dimers (like the dimer shown in (c)) is ruled out as this could only produce one set of Asn resonances. **b**, An equilibrium between trimers would also account for two sets of Asn NMR signals. **c**, An equilibrium between dimer and trimer would require that one of the three species present (monomer, dimer or trimer) be undetectable by NMR. It should be noted that in modeling studies of the soluble trimeric leucine zipper³¹, distances between Asn side chains only supported a subset of possible interhelical hydrogen bonds.

NMR data also show evidence of helical secondary structure, consistent with the CD results. Although there exists significant degeneracy in most of the leucine and valine signals, two distinct helical NH(i)–NH(i+1) NOE connectivity patterns are resolved. The NHs at 7.4 p.p.m. that are in dipolar contact with the Asn side chains give rise to TOCSY (total correlation spectroscopy) peaks at 3.2 p.p.m., which are assigned as α Hs. These α Hs also have strong NOEs to the Asn N δ protons and weak NOEs to the longest of the resolved helical NOE patterns (that is, the pattern that begins at 8.8 p.p.m.) indicating that the asparagines are located in proximity to a region of helical secondary structure.

The asymmetric hydrogen bonding pattern of the interfacial asparagine in soluble leucine zippers has been identified in X-ray structures¹⁴ and studied by NMR³⁵. In the soluble Jun leucine zipper, NMR data showed that the temperature where significant conformational averaging occurs is $\sim 5^\circ\text{C}$ (ref. 35). The disappearance of NMR signals below this temperature was attributed to the intermediate time scale of the Asn side chains between the asymmetric conformations seen in the X-ray structure¹⁴. A similar feature has been reproduced in our designed leucine zipper membrane protein. Preliminary proton NMR data show two distinct asparagine NOE patterns, revealing that there are two side chain conformations at low temperatures and that they undergo conformational exchange as the temperature increases until averaging is achieved at $>20^\circ\text{C}$. In contrast to the NMR study of the soluble leucine zipper, we can actually detect the species where the side chains are locked into distinct conformations. This can only be caused by a restriction of the side chain by either packing or hydrogen bonding interactions. The observation of two side chain conformations not exchanging in the NMR time scale is quite unusual. Although we do not yet have enough NMR constraints to predict a high-resolution model for the structure of the Asn side chain, the crystal structure of the soluble protein is one possibility (Fig. 8a)¹⁴. Other possible models are shown in Fig. 8b,c. Both dimers and trimers are possible because the NMR data alone do not provide information on the oligomeric state. In addition, we have found that the propensity to form dimer *versus* trimer depends on the conditions of study.

Structural studies are underway which will allow us to more thoroughly define the membrane leucine zipper interface and address whether the peptides form a coiled coil.

Biological implications of polar residues

Transmembrane helices are characterized by long stretches of hydrophobic residues with few or no polar side chains³⁶. The paucity of polar residues in transmembrane helices, compared to other proteins, has been reasoned in terms of energetic costs of inserting polar groups into a hydrophobic environment^{2,36}. Although functionally necessary, polar groups present a danger — if polar residues are present and required for functions of membrane proteins, strong interhelical hydrogen bonds in membranes could increase the probability of unintended and unregulated association of transmembrane helices. Thus, folding of membrane proteins may be regulated to permit sequestration of polar groups in the interior of these proteins, perhaps through transmembrane chaperones analogous to those in aqueous compartments. Biological consequences of unregulated helix associations could be disastrous. For example, mutation of a valine to a glutamic acid in the neu oncogene transmembrane domain results in specific dimer formation and constitutive activation of this protein, leading to a lethal phenotype^{37–39}. It was further determined that a hydrogen bond is formed between the protonated carboxyl moieties⁴⁰. Changes in helix association stability and specificity involving polar interactions in membranes may reveal other mechanisms of disease.

Methods

Construction of Staphylococcal nuclease chimeric proteins.

All plasmids encoding nuclease chimeras were constructed from pT7SN/GpA99 (ref. 3). The GpA sequence was removed from pT7SN/GpA99 by polymerase chain reaction (PCR) mutagenesis in the *HindIII*–*BamHI* region of the plasmid. A unique *AvrII* site at the end of the linker was created at the same time. The *AvrII*–*BamHI* fragments encoding LLLL or VNVV were made by annealing and extending two oligonucleotides complementary at their 3' ends followed by PCR amplification. pT7SN/VVVV was generated from pT7SN/VNVV by site-directed mutagenesis (QuickChangeTM, Stratagene). Annealing the 5' oligonucleotide for the VNVV fragment with the 3' oligonucleotide for the LLLL fragment and subsequent PCR amplification by the primers for VNVV resulted in two

other *AvrII-BamHI* fragments encoding VNVL and VNLL TM designs. The VNVL and VNLL fragments and pT7SN/VNVV were mutated and amplified by PCR using primers for LLLL, giving *AvrII-BamHI* fragments for LNVL, LNLL and LNVV, respectively. These five fragments were inserted into the pT7SN/linker to create their corresponding nuclease chimeras.

Construction of TOXCAT chimeras. The construction of pccKAN and chimera of GpA has been described¹⁰. To create the chimeras for NV, VN, NN and VV, an oligonucleotide with degenerate codons at the two a positions was PCR amplified, and cloned into pccKAN as an *NheI-BamHI* fragment. The LL construct was obtained by PCR amplification of the poly-leucine sequence from pT7SN/LLLL and subcloning into pccKAN.

VNVV peptide synthesis and purification. Solid phase synthesis of the peptide was performed using a Fmoc chemistry⁴¹ on an Applied Biosystems 431A Peptide synthesizer. Amino acids and polyethylene glycol (PEG) resin were obtained from either PerSeptive Biosystems or Advanced ChemTech. Deprotection and cleavage reactions were carried out in trifluoroacetic acid (TFA) with 5% (v/v) each of ethanedithiol, phenol, ethyl methyl sulfide, thioanisole and water for four hours. Cleaved peptide was concentrated and subsequently precipitated in ice-cold ethyl ether. This deprotection/cleavage procedure was repeated on the resulting precipitate to completely deprotect the side chains. The peptide was purified by a semipreparative YMC HPLC phenyl column and eluted in a 50–100% organic gradient (2:3 acetonitrile:isopropanol) containing 0.05% TFA. Fractions containing the peptide were determined by mass spectrometry and were lyophilized promptly to remove residual TFA. The lyophilized peptide can be readily redissolved in water or buffer with detergent (2–5%). The concentration and chemical composition of the peptide were obtained by amino acid analysis (Keck Biotechnology Resource Laboratory, Yale University).

Expression and purification of nuclease chimeras. Plasmids were transformed into *E. coli* HMS174(DE3) cells (Novagen). Bacterial growth, induction, harvest, lysis and protein extraction were performed according to Lemmon *et al.*³, except that Thesit (Boehringer Mannheim Inc.) was used in place of Lubrol PX. Purification was also based on protocols previously described³ with the following modifications. After extraction, the suspension was centrifuged in a JA-20 rotor (Beckman) at 8,000 r.p.m. for 30 min. Chimeric proteins in the supernatant were pure enough to be analyzed for association in SDS-PAGE. For further purification, the proteins were dialyzed for 4 hours at 4 °C against 25 mM TrisHCl, 1 mM ethylenediaminetetraacetate (EDTA), 200 mM NaCl and 0.2% (w/v) Thesit to lower the salt concentration for the subsequent anion- and cation-exchange chromatography. The dialyzed sample was mixed with pre-equilibrated DEAE resin (Sigma). The nuclease chimera in the aqueous phase was separated from the DEAE resin by centrifugation and then bound to SP resin (EM Science). The SP resin was washed twice with 20 volumes of 25 mM TrisHCl, 1 mM EDTA, 220 mM NaCl, 100 mM phenylmethylsulfonyl fluoride (PMSF), 0.025% Na₂S₂O₃ and 0.2% Thesit (w/v). Finally, the protein was eluted in 25 mM TrisHCl, 1 mM EDTA, 1 M NaCl, 100 mM PMSF, 0.025% Na₂S₂O₃, 0.2% Thesit, and 0.7% of SDS (w/v). The purified chimeras were concentrated with Ultrafree Centrifugal Filters (Millipore Corp) and concentrations determined by bicinchoninic acid assays (Pierce). Purified GpA chimeric protein was kindly provided by Dr. Zimei Bu (National Institute of Standard and Technology).

Expression of TOXCAT chimeras and CAT assays. Plasmids containing TOXCAT chimeras were transformed into *E. coli* NT326

(*MalE*) cells (kindly provided by H. Shuman, Columbia University), which constitutively expresses these chimeric proteins at low levels. Cells were grown in Luria-Bertani medium with 200 mg l⁻¹ of ampicillin. *malE* complementation, CAT (Quant-T-CAT, Amersham) and disk diffusion assays were carried out as described¹⁰. Whole cell lysates were used to estimate expression levels of chimeras and were detected by immunoblotting against MBP. Anti-MBP antibodies were obtained from New England Biolab. Immunoblots were developed using the ECL kit (Amersham) and band intensities were quantified using densitometry. To detect chimeras in the membrane fraction, cells were resuspended in 50 mM TrisHCl, 5 mM EDTA, 1 mM PMSF and 0.025% Na₂S₂O₃ (w/v), and lysed by three rounds of freeze/thaw cycles and multiple passages through a 30G syringe needle. The membrane and soluble fractions were separated by centrifugation. The presence of chimeras in the membrane fractions was detected by SDS-PAGE followed by immunoblotting against MBP.

Gel electrophoresis. SDS-PAGE of nuclease chimeras along with the molecular weight standard (BioRad) was performed in homogeneous 20% PhastGels (Pharmacia) and stained with Coomassie brilliant blue. Purified chimeras in SDS were analyzed at a concentration of 25 µM. Samples were not boiled prior to electrophoresis since results were found to be independent of boiling. Competition experiments required premix of the VNVV peptide in SDS with purified chimeric proteins. For immunoblotting TOXCAT chimeras, SDS-PAGE of cell lysates was performed in 10% minigels (BioRad).

NMR spectroscopy. 0.79 mg of HPLC purified synthetic membrane leucine zipper ($M_w = 3,272$ Da) were dissolved into 0.3 ml of 100 mM d₂₅-SDS (Cambridge Isotopes), 100 mM Sodium phosphate, pH 6.0, 10% D₂O. NMR spectra were collected on Varian Inova 500 and 800 MHz spectrometers. Water suppression was achieved using RAWatergate^{42,43}; the total time for the water suppression echo was 5.0 ms. One-dimensional spectra (16 k complex data points, 500 MHz spectral width = 7000 Hz; 800 MHz spectral width = 10,000 Hz were referenced externally at each temperature to dioxane at 3.75 p.p.m. Two-dimensional NOESY ($\tau_{mix} = 35$ ms) and TOCSY ($\tau_{mix} = 45$ ms) spectra were acquired at 10 °C and 45 °C on the 800 MHz spectrometer. The matrices were 4096 × 256 (zero-filled to 512) complex data points with a spectral width of 9000 Hz in each dimension. All data were processed with gaussian window functions (1D: inverse exponential 25 Hz, gaussian width 18 Hz; 2D: inverse exponential 30 Hz (t₂), 15 Hz (t₁), gaussian width 45 Hz (t₁, t₂)) using NMRPipe⁴⁴.

CD spectroscopy. 15 µl of the NMR sample were diluted into 900 µl of 10 mM SDS, 100 mM sodium phosphate, pH 6.0. Data were collected on an Aviv 62DS spectrometer, using a cuvette of 2 mm path length. Thermal melts were performed by collecting data at 222 nm every 2 °C (0.5 min equilibration time) with an averaging time of 2 s.

Acknowledgments

We thank P.D. Adams, K. R. MacKenzie, A. Senes and I. Ubarretxena for helpful discussions. We are also indebted to L. Fisher for advice and assistance in peptide synthesis. We kindly acknowledge G. King for permission to adapt a figure. This research is funded with a program project grant on helix interactions in membrane proteins (National Institute of Health) and the National Foundation for Cancer Research.

Received 11 November, 1999; accepted 20 December, 1999.

1. Popot, J.-L. & Engelman, D.M. Membrane protein folding and oligomerization: the two-stage model. *Biochemistry* **29**, 4031–4037 (1990).
2. Engelman, D.M. & Steitz, T.A. On the folding and insertion of globular membrane proteins. in *The protein folding problem* (ed. Wetlauffer, D.B.) 87–113 (Westview, Boulder, Colorado, 1984).
3. Lemmon, M.A. et al. Glycophorin A dimerization is driven by specific interactions between transmembrane α -helices. *J. Biol. Chem.* **267**, 7683–7689 (1992).
4. Lemmon, M.A., Flanagan, J.M., Treutlein, H.R., Zhang, J. & Engelman, D.M. Sequence specificity in the dimerization of transmembrane α -helices. *Biochemistry* **31**, 12719–12725 (1992).
5. Lemmon, M.A., Treutlein, H.R., Adams, P.D., Brunger, A.T. & Engelman, D.M. A dimerization motif for transmembrane α -helices. *Nature Struct. Biol.* **1**, 157–163 (1994).
6. Treutlein, H.R., Lemmon, M.A., Engelman, D.M. & Brunger, A.T. The glycophorin A transmembrane domain dimer: sequence-specific propensity for a right-handed supercoil of helices. *Biochemistry* **31**, 12726–12733 (1992).
7. Langosch, D., Brosig, B., Kolmar, H. & Fritz, H.-J. Dimerisation of the glycophorin A transmembrane segment in membranes probed with the ToxR transcription activator. *J. Mol. Biol.* **525**–530 (1996).
8. MacKenzie, K.R., Prestegard, J.H. & Engelman, D.M. A transmembrane helix dimer: structure and implications. *Science* **276**, 131–133 (1997).
9. MacKenzie, K.R. & Engelman, D.M. Structure-based prediction of the stability of transmembrane helix-helix interactions: the sequence dependence of glycophorin A dimerization. *Proc. Natl. Acad. Sci. USA* **95**, 3583–3590 (1998).
10. Russ, W.P. & Engelman, D.M. TOXCAT: a measure of transmembrane helix association in a biological membrane. *Proc. Natl. Acad. Sci. USA* **96**, 863–868 (1999).
11. Fleming, K.G., Ackerman, A.L. & Engelman, D.M. The effect of point mutations on the free energy of transmembrane α -helix dimerization. *J. Mol. Biol.* **272**, 266–275 (1997).
12. Deisenhofer, J., Epp, O., Miki, K., Huber, R. & Michel, H. Structure of the protein subunits in the photosynthetic reaction centre of *Rhodospseudomonas viridis* at 3 Å resolution. *Nature* **318**, 618–624 (1985).
13. Henderson, R. et al. Model for the structure of bacteriorhodopsin based on high-resolution electron cryo-microscopy. *J. Mol. Biol.* **213**, 899–929 (1990).
14. O'Shea, E.K., Klemm, J.D., Kim, P.S. & Alber, T. X-ray structure of the GCN4 leucine zipper, a two-stranded, parallel coiled coil. *Science* **254**, 539–544 (1991).
15. Jones, D.T., Taylor, W.R. & Thornton, J.M. A mutation data matrix for transmembrane proteins. *FEBS Lett.* **339**, 269–275 (1994).
16. Samatey, F.A., Xu, C. & Popot, J.-L. On the distribution of amino acid residues in transmembrane α -helix bundles. *Proc. Natl. Acad. Sci. USA* **92**, 4577–4581 (1995).
17. Arkin, I.T. & Brunger, A.T. Statistical analysis of predicted transmembrane α -helices. *Biochim. Biophys. Acta* **1429**, 113–128 (1998).
18. Arkin, I. et al. Structural organization of the pentameric transmembrane α -helices of phospholamban, a cardiac ion channel. *EMBO J.* **13**, 4757–4764 (1994).
19. Kolmar, H. et al. Membrane insertion of the bacterial signal transduction protein ToxR and requirements of transcription activation studied by modular replacement of different protein substitution. *EMBO J.* **14**, 3895–3904 (1995).
20. Harbury, P.B., Zhang, T., Kim, P.S. & Alber, T. A switch between two-, three- and four-stranded coiled coils in GCN4 leucine zipper mutants. *Science* **262**, 1401–1407 (1993).
21. Lovejoy, B. et al. Crystal structure of a synthetic triple-stranded α -helical bundle. *Science* **259**, 1288–1293 (1993).
22. Zhu, B.-Y., Zhou, N.E., Kay, C.M. & Hodges, R.S. Packing and hydrophobicity effects on protein folding and stability: Effects of β -branched amino acids, valine and isoleucine, on the formation of stability of two-stranded α -helical coiled coils/leucine zippers. *Protein Sci.* **2**, 383–394 (1993).
23. Zhou, N.E., Kay, C.M. & Hodges, R.S. The role of interhelical ionic interactions in controlling protein folding and stability: De novo designed synthetic two-stranded α -helical coiled coils. *J. Mol. Biol.* **237**, 500–512 (1994).
24. Zhou, N.E., Kay, C.M. & Hodges, R.S. The net energetic contribution of interhelical electrostatic attractions to coiled-coil stability. *Protein Eng.* **7**, 1365–1372 (1994).
25. Lumb, K.J. & Kim, P.S. A buried polar interaction imparts structural uniqueness in a designed heterodimeric coiled coil. *Biochemistry* **34**, 8642–8648 (1995).
26. Gurezka, R., Laage, R., Brosig, B. & Langosch, D. A heptad motif of leucine residues found in membrane proteins can drive self-assembly of artificial transmembrane segments. *J. Biol. Chem.* **274**, 9265–9270 (1999).
27. Potekhin, S.A., Medvedkin, V.N., Kashparov, I.A. & Venyaminov, S.Y. Synthesis and properties of the peptide corresponding to the mutant form of the leucine zipper of the transcriptional activator GCN4 from yeast. *Protein Eng.* **7**, 1097–1101 (1994).
28. Vieth, M., Kolinski, A. & Skolnick, J. Method for predicting the state of association of discretized protein models: Applications to leucine zippers. *Biochemistry* **35**, 955–967 (1996).
29. Zeng, X., Herndon, A.M. & Hu, J.C. Buried asparagines determine the dimerization specificities of leucine zipper mutants. *Proc. Natl. Acad. Sci. USA* **94**, 3673–3678 (1997).
30. Choma, C., Gratkowski, H., Lear, J.D. & DeGrado, W.F. A membrane-soluble analogue of the two-stranded coiled coil from GCN4. *Nature Struct. Biol.* **7**, 161–166 (2000).
31. Gonzalez, L., Woolfson, D.N. & Alber, T. Buried polar residues and structural specificity in the GCN4 leucine zipper. *Nature Struct. Biol.* **3**, 1011–1018 (1996).
32. Gonzalez, L., Brown, R.A., Richardson, D. & Alber, T. Crystal structures of a single coiled-coil peptide in two oligomeric states reveal the basis for structural polymorphism. *Nature Struct. Biol.* **3**, 1002–1010 (1996).
33. Gonzalez, L., Plecs, J.J. & Alber, T. An engineered allosteric switch in leucine zipper oligomerization. *Nature Struct. Biol.* **3**, 510–515 (1996).
34. Drees, B.L., Grotkopp, E.K. & Nelson, H.C.M. The GCN4 leucine zipper can functionally substitute for the heat shock transcription factor's trimerization domain. *J. Mol. Biol.* **273**, 61–74 (1997).
35. Junius, F.K. et al. Nuclear magnetic resonance characterization of the Jun leucine zipper domain: unusual properties of coiled-coil interfacial polar residues. *Biochemistry* **34**, 6164–6174 (1995).
36. Engelman, D.M., Steitz, T.A. & Goldman, A. Identifying nonpolar transbilayer helices in amino acid sequences of membrane proteins. *Annu. Rev. Biophys. Chem.* **15**, 321–353 (1986).
37. Bargmann, C.I., Hung, M.-C. & Weinberg, R.A. Multiple independent activations of the neu oncogene by a point mutation altering the transmembrane domain of p185. *Cell* **45**, 649–657 (1986).
38. Weiner, D.B., Liu, J., Cohen, J.A., Williams, W.V. & Greene, M.I. A point mutation in the neu oncogene mimics ligand induction of receptor aggregation. *Nature* **339**, 230–231 (1989).
39. Hynes, N.E. & Stern, D.F. The biology of erbB-2/neu/HER-2 and its role in cancer. *Biochim. Biophys. Acta* **1198**, 165–184 (1994).
40. Smith, S.O., Smith, C.S. & Bormann, B.J. Strong hydrogen bonding interactions involving a buried glutamic acid in the transmembrane sequence of the neu/erbB-2 receptor. *Nature Struct. Biol.* **3**, 252–258 (1996).
41. Fields, G.B. & Noble, R.L. Solid phase peptide synthesis utilizing 9-fluorenylmethoxycarbonyl amino acids. *Int. J. Peptide Protein Res.* **35**, 161–214 (1990).
42. Piotta, M., Saudek, V. & Sklenar, V. Gradient-tailored excitation for single-quantum NMR spectroscopy of aqueous solutions. *J. Biomol. NMR* **2**, 661–665 (1992).
43. Altieri, A. & Byrd, R.A. Randomization approach to water suppression in multidimensional NMR using pulsed field gradients. *J. Magn. Reson.* **107B**, 260–266 (1995).
44. Delaglio, F. et al. NMRPipe: a multidimensional spectral processing system based on UNIX pipes. *J. Biomol. NMR* **6**, 277–293 (1995).